Field evidence of pressure gradient induced incipient motion

D. L. Foster,[1] A. J. Bowen,[2] R. A. Holman,[3] and P. Natoo[1]

Received 31 December 2004; revised 17 November 2005; accepted 19 January 2006; published 4 May 2006.

[1] Recently, models for the onshore migration of nearshore sandbars were improved by including an empirical acceleration term in the sediment transport formulation (Hoefel and Elgar, 2003). Here, field observations of the fluid-sediment interface suggest that the success of this empirical parameter may result from unsteady forcing of sediment beds by nearshore waves. The velocity and sediment observations show that, under large pressure gradients present during the strengthening of onshore-directed flow, several centimeters of previously still sediment can be mobilized and transported onshore. The onshore-directed mobile-bed layer rapidly settles as the wave velocity weakens. These observations are inconsistent with traditional sediment transport theories (Shields, 1936; Bagnold, 1966) that assume incipient motion is solely based on the force applied by bed stress but are consistent with theories that include an additional force induced by the horizontal pressure gradient (Madsen, 1974; Sleath, 1999). In this paper, we provide the first field evidence of incipient motion that is significantly influenced by the unsteady forcing introduced by the horizontal pressure gradient due to surface gravity waves.

Citation: Foster, D. L., A. J. Bowen, R. A. Holman, and P. Natoo (2006), Field evidence of pressure gradient induced incipient motion, *J. Geophys. Res.*, *111*, C05004, doi:10.1029/2004JC002863.

1. Introduction

[2] Decades of observations have shown that surf-zone sandbars respond to large waves and currents produced by offshore storm events by migrating offshore in hours to days. The beach rebuilds more slowly (weeks to months) with onshore migration of sandbars under moderate-waves and small mean currents. Commonly used energetics-based sediment transport models predict the offshore migration of sandbars with significant skill [*Thornton et al.*, 1996; *Gallagher et al.*, 1998]. However, the simulation of onshore migration events results in poor model skill. Model performance has recently been improved through the inclusion of an empirically-based fluid-acceleration parameter [*Drake and Calantoni*, 2001; *Hoefel and Elgar*, 2003]. One possible explanation for the success of the empirical fluid-acceleration parameter is that the additional term compensates for the simplifying assumptions required for the quadratic stress law assumed in energetics-based sediment transport models [*Bagnold*, 1966; *Bowen*, 1980; *Bailard*, 1981; *Henderson et al.*, 2004]. An additional explanation is that under certain conditions, the incipient motion of sediment may also be induced by a horizontal pressure gradient applied to the seabed by surface gravity waves and not, as is commonly assumed, the force applied by the vertical gradient of shear stress.

[3] Even in steady flow (i.e., rivers), understanding the mechanics of moving sediment remains a challenge for scientists and engineers. In a coastal environment, this process is complicated by combined (oscillatory, steady, and turbulent) flows (for a review, please see *Fredsøe and Deigaard* [1992] and *Nielsen* [1992]). Traditionally, the incipient motion and near-bed transport of sediment is parameterized with the Shields parameter [*Shields*, 1936], which represents the ratio of the mobilizing force applied by the shear stress over a single layer of grains to the stabilizing force applied by gravity. Here, we define this parameter in a time-dependent form given by

$$\theta(t) = \frac{\tau_b(t)}{(\rho_s - \rho) g d_{50}} \tag{1}$$

where τ_b is the instantaneous applied bed stress, ρ_s is the sediment density, ρ is the water density, g is gravity, and d_{50} is the grain size diameter. At the critical limit, the Shields parameter represents the vertical gradient of the shear stress applied over a single grain thickness. Transport models assume incipient motion occurs when some critical bed stress is exceeded ($|\theta| > 0.03 \sim 0.06$) and parameterize the sediment concentration as a function of the excess stress [*Engelund and Fredsøe*, 1976; *Zyserman and Fredsøe*, 1994; *Hanes and Bowen*, 1985]. As stress increases, ripples develop and sediment is easily suspended. As stress further increases ($|\theta| > 0.8 \sim 1.0$), ripples are washed out and a thicker mobile-bed layer develops. This mobile-bed layer is called sheet-flow and is approximately 10∼60 grain

[1]Department of Civil and Environmental Engineering and Geodetic Science, Ohio State University, Columbus, Ohio, USA.
[2]Department of Oceanography, Dalhousie University, Halifax, Nova Scotia, Canada.
[3]College of Oceanic and Atmospheric Sciences, Oregon State University, Corvallis, Oregon, USA.

0148-0227/06/2004JC002863$09.00

diameters thick [*Bagnold*, 1966; *Dohmen-Janssen et al.*, 2001; *Hsu and Hanes*, 2004]. Observations of sheet-flow thickness in a large-scale wave flume showed a linear increase in the thickness with the Shields parameter [*Dohmen-Janssen and Hanes*, 2002, 2005] and were consistent with the predictions by *Sumer et al.* [1996]. The observations showed that skewed waves with peak Shields parameters of 0.8∼1.0 resulted in sheet-flow thickness of 10∼20 grain diameters. When wave groups with asymmetric wave forms (i.e., saw-toothed) were examined, this thickness increased to 30 grain diameters.

[4] Recent laboratory and theoretical investigations indicate that when the overlying wave acceleration is large, the bed may temporarily dilate resulting in a significantly larger (O(cm)) mobile-bed layer [*Sleath*, 1999]. In a series of oscillatory laboratory tunnel experiments, bed dilation occurred when the horizontal pressure gradient applied to individual sediment grains dominates the immersed weight of the grains [*Dick and Sleath*, 1991; *Sleath*, 1994; *Zala Flores and Sleath*, 1998]. The horizontal pressure gradient for sinusoidal waves generated in the tunnel is $p_x(t) = \rho U_o \omega \sin(\omega t)$, where ω is the angular wave frequency, U_o is the velocity amplitude, and the subscript x infers differentiation by x. *Sleath* [1999] characterized the role of the pressure gradient in incipient motion with a ratio between the destabilizing force applied by the peak horizontal pressure gradient to the stabilizing force applied by gravity. This non-dimensional Sleath parameter was defined with

$$S_\omega = \frac{\rho U_o \omega}{(\rho_s - \rho) g}. \quad (2)$$

Unlike the Shields parameter, the Sleath parameter has no dependence on the grain size. The laboratory observations indicate that plug flow occurs when the Sleath parameter exceeds a critical value of 0.29. More recently, laboratory observations of coarse particles under regular shoaling waves suggest that incipient motion of the particles results from the combined effect the bed shear and the pressure gradient [*Terrile et al.*, 2005].

[5] Theories regarding mobile-bed sediment layers have largely been evaluated in qualitative field investigations [*Conley and Inman*, 1992] or in controlled laboratory experiments [*Horikawa et al.*, 1982; *Dick and Sleath*, 1991; *Ribberink and Chen*, 1993; *Dohmen-Janssen et al.*, 2001; *Dohmen-Janssen and Hanes*, 2002]. Observations for testing fully unsteady mobile-bed theories have thus far only occurred in oscillatory laboratory tunnels [*Dick and Sleath*, 1991; *King*, 1991; *Ribberink and Chen*, 1993; *Zala Flores and Sleath*, 1998]. In this paper, we provide the first known field observations that show the temporary mobilization of the bed and support the existence of pressure gradient induced transport.

2. Results

[6] A 1994 investigation at the Army Corps of Engineers Field Research Facility (FRF), Duck94, NC, provided the first quantitative field observations of the bed load/sheet-flow layer. This experiment consisted of a vertical array of 4 hot-film anemometers for measuring flow and a stacked array of 19 fiber-optic backscatter (FOBS) probes for measuring sediment concentration [*Foster et al.*, 2000]. The instrument array was deployed on the seaward edge of the bar crest in a water depth of 1.5 m. The vertical array of hot-film anemometers measured the vertical and temporal structure of the wave bottom boundary layer over a flat bed of coarse-grained sediment (d_{50} = 0.2 mm). Several of the sediment concentration probes pierced the bed and measured the bed elevation at 1 cm increments. Both observations of the phase shift of the wave bottom boundary layer velocity relative to the free-stream and estimations of the bed shear stress were significantly smaller than those predicted by an eddy viscosity model that assumes a rough immobile bed [*Foster et al.*, 2000].

[7] During the experiment, the hot-film sensors became intermittently buried for approximately 256-seconds. Sensors that were intermittently buried during low flow recorded significant onshore velocities initiated during large accelerations present prior to large wave crests (Figure 1). A 30-second time series of velocity and concentration shows three intermittently buried hot-film sensors that record four events with significant onshore velocities (Figure 1b). Consistent with the laboratory observations [*Zala Flores and Sleath*, 1998] and theoretical predictions [*Madsen*, 1974; *Sleath*, 1999], several centimeters of sediment, at rest under the wave trough, are temporarily mobilized. The mobilizations are initiated during the large accelerations present during flow reversal from offshore- to onshore-directed flow. The bed rapidly settles during the deceleration following the wave crests approximately 1∼2 seconds later. During these four events, two of the intermittently buried hot-films record instantaneous velocities of as large as 100 cm/s. Two of these events (1358 s and 1363 s) are coincident with a decrease in concentration of the lowest intermittently buried fiber-optic backscatter probe (Figure 1d). The events precede suspended sediment plumes that occur during the weakening flow phase following the wave crest (Figure 1c). A physical explanation for this previously unobserved phenomena is that the sensors were observing plug flow where the pressure gradients associated with large wave crests mobilized up to 2∼3 cm of the otherwise fixed bed.

[8] A closer examination of two wave sequences shows significant differences between small waves with velocity amplitudes, U_o, of approximately 50 cm/s and large waves with velocity amplitudes of approximately 100 cm/s (Figure 2). Vertical profiles of velocity (low pass filtered at 2 Hz and displayed at 0.25 s intervals) validate the no-slip condition during a smaller wave through both a transition to onshore-directed flow (Figure 2b) and a transition to offshore-directed flow (Figure 2c). However, the larger wave sequence shows significant bed response during the transition to onshore-directed flow (Figure 2d). In less than 1-second, the previously undisturbed bed experiences a low pass filtered flow of 50 cm/s. Following the passage of the wave crest, the bed rapidly returns to its undisturbed state (Figure 2e).

[9] In shallow coastal waters, the random waves propagating towards the surf-zone become skewed (shorter-duration larger-amplitude crests and longer-duration smaller-amplitude wave troughs) and asymmetric (pitched forward with a sawtooth shape) [*Elgar and Guza*, 1985]. Maximum acceleration is reached under the wave crests prior to breaking. We generalize Sleath's parameter, S, to an

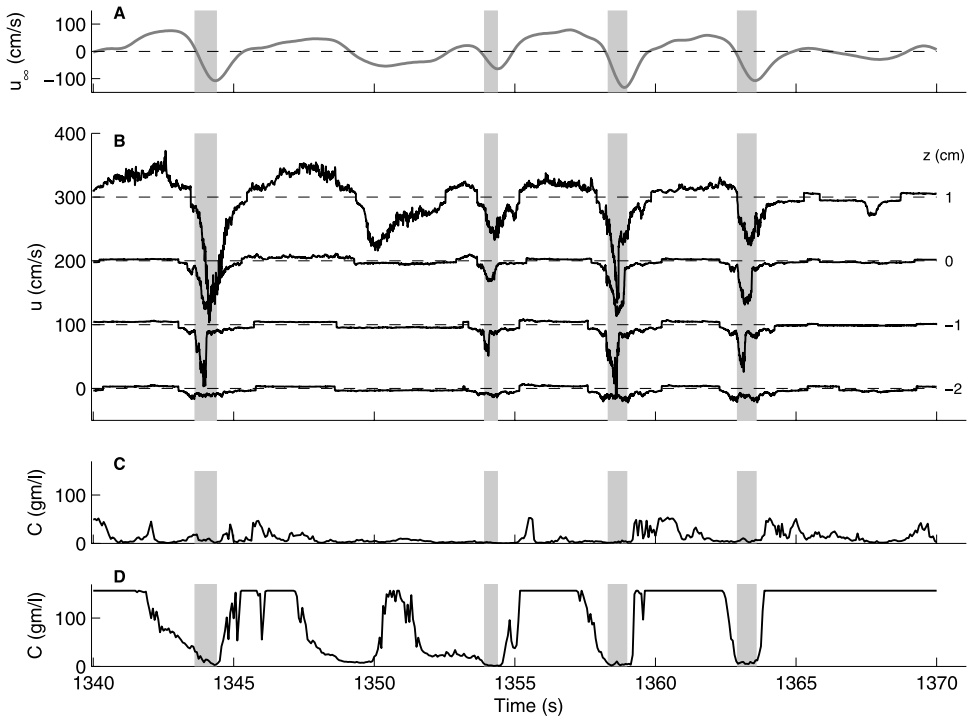

Figure 1. A 30-second time series of velocity and concentration observations showing four temporary bed mobilizations. (a) The free-stream velocity measured at 10.5 cm above the bed was resolved to 2 Hz. Positive velocity is directed offshore. (b) The velocity measured at 4 positions above and within the intermittently mobile-bed bed was resolved to 200 Hz. Each velocity record is offset by 100 cm/s. Sensor elevations relative to still bed are given to the right of each time series. (c and d) The sediment concentration measured at 3 cm and 0 cm, respectively, above the undisturbed bed elevation. The gray shaded areas highlight the strengthening flow phase of the onshore-directed flow of the 4 mobile-bed events.

instantaneous Sleath parameter explicitly defined with the pressure gradient as

$$S(t) \equiv \frac{-p_x(t)}{(\rho_s - \rho)g}. \tag{3}$$

In shallow water wave environments, the horizontal pressure gradient becomes $-p_x = \rho(u_\infty)_t + \rho u_\infty(u_\infty)_x$, where u_∞ is the free-stream wave velocity and the subscript t infers differentiation by t. Approximating the pressure gradient in the boundary layer with linear wave theory results in $-p_x = \rho(u_\infty)_t$. Here, the instantaneous Sleath parameter is approximated with the acceleration of the free-stream velocity and is defined by

$$S(t) = \frac{\rho u_{\infty_t}}{(\rho_s - \rho)g} \tag{4}$$

For the offshore positive sign convention in the Duck94 observations, the sign of this quantity will identify strengthening onshore-directed flow with a negative magnitude and strengthening offshore-directed flow with a positive magnitude.

[10] During the 30-second window, the instantaneous parameter, $S(t)$ reaches its largest local maxima during both the acceleration and deceleration phases of the onshore-directed flow (Figure 3). The bed mobilizations were coincident with the slightly larger negative peaks in S(t) during the accelerating phase of the onshore-directed flows. A cross-spectral analysis between $S(t)$ and $u(z = 10.5)$ showed that the Sleath parameter leads the free-stream velocity by 88° at the incident wave frequency of 0.2 Hz. The critical value of the Sleath parameter suggested by laboratory experiments ($|S_\omega| > 0.29$) was approached during the onset of the mobilizations but never exceeded (Figure 3c). The mobilizations occurred for $|S(t)| > 0.1$, suggesting a lower critical limit for natural beds exposed to surface gravity waves.

[11] Numerical predictions of the bed stress and Shields parameter (equation (1)) were estimated with a two-dimensional Reynolds Averaged Navier Stokes (RANS) model. The equations are closed with a k-ω turbulence closure model. The k-ω model avoids the use of wall functions and has been shown to perform better than the k-ϵ model in regions of adverse pressure gradients present in rippled bed geometries [*Wilcox*, 1993]. This model has been successfully used to resolve the flow field over ripples in both pure wave and combined wave-current flows [*Fredsøe et al.*, 1999; *Chang and Hanes*, 2004]. The model is forced with an oscillatory pressure gradient approximated with linear wave theory and estimated with the local horizontal acceleration of the uppermost horizontal velocity record at z = 10.5 cm. The computational domain was resolved with 100 vertical grid points and 3 horizontal grid points. Periodicity is assumed at the lateral boundaries and symmetry is assumed at the upper boundary. A no-slip boundary

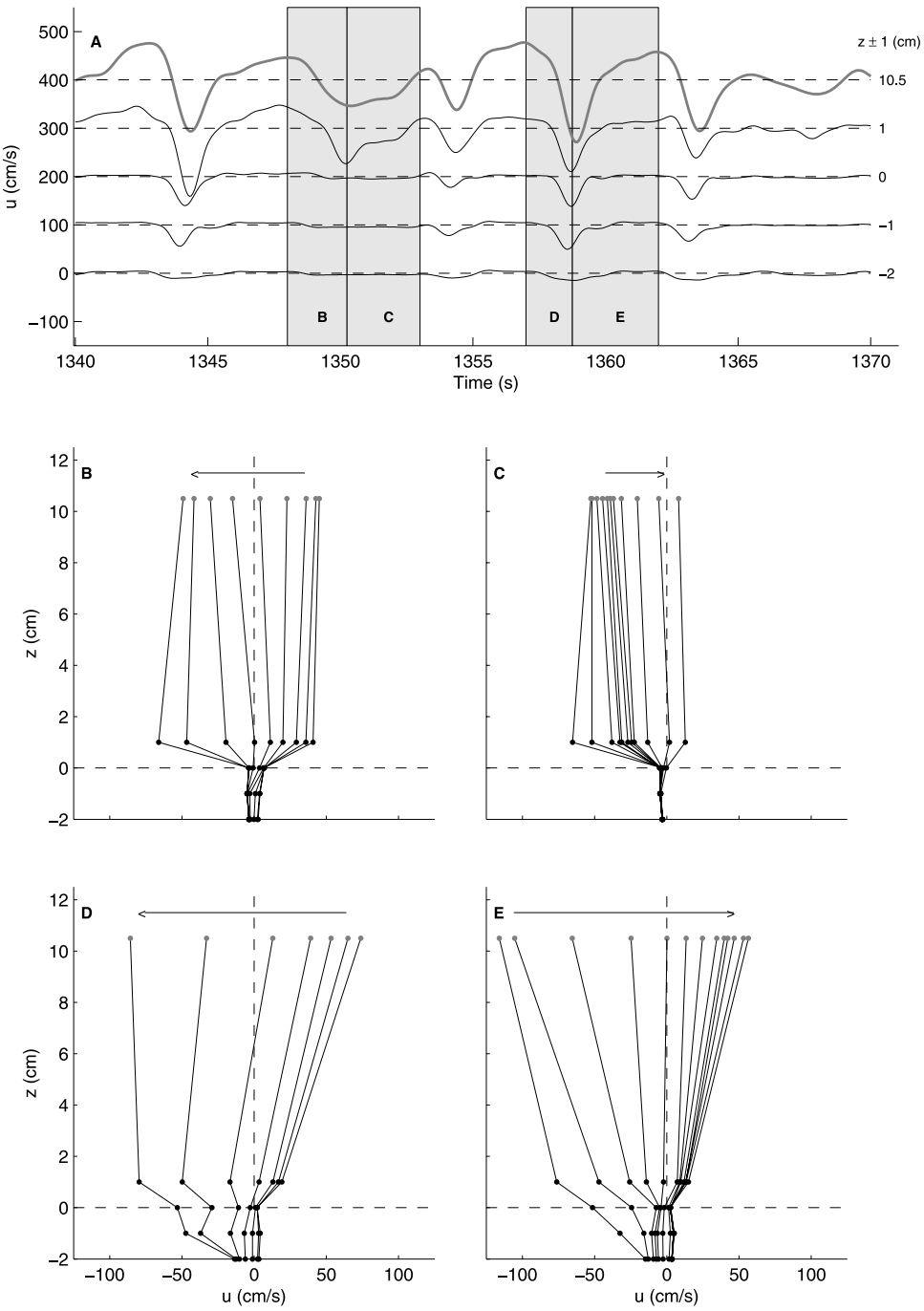

Figure 2. Vertical profiles of horizontal velocity for two wave sequences. (a) The velocity observations are low pass filtered at 2 Hz. Each velocity record is offset by 100 cm/s. The gray shaded areas indicate the temporal range of the vertical profiles displayed in Figures 2b–2e. (b–e) The vertical profile of the low pass filtered velocity is shown at 0.25 s intervals. The undisturbed bed elevation is given with the green dashed line. The direction of the arrows indicate the direction of wave propagation during each time sequence. Figures 2b and 2c show the vertical profile of velocity for a small 5-second wave with a peak free-stream velocity of 50 cm/s, where the bed remains undisturbed. Figures 2d and 2e show the vertical profile of velocity for a larger 5-second wave with a peak free-stream velocity of 100 cm/s, where more than 2 cm of previously settled sediment is mobilized.

condition is assumed at the undisturbed bed elevation $u(z = k_s/30)$, where k_s is the Nikuradse bed roughness equivalent to a 0.2 mm flat sand bed ($k_s = 2.5d_{50}$). Please see *Fredsøe et al.* [1999] for further model specifics.

[12] The skewed wave field results in an asymmetric bed stress with larger amplitudes generally observed during the onshore-directed flows (Figure 3d). The bed stress leads the horizontal velocity at $z = 10.5$ cm by 14°. This phase shift is

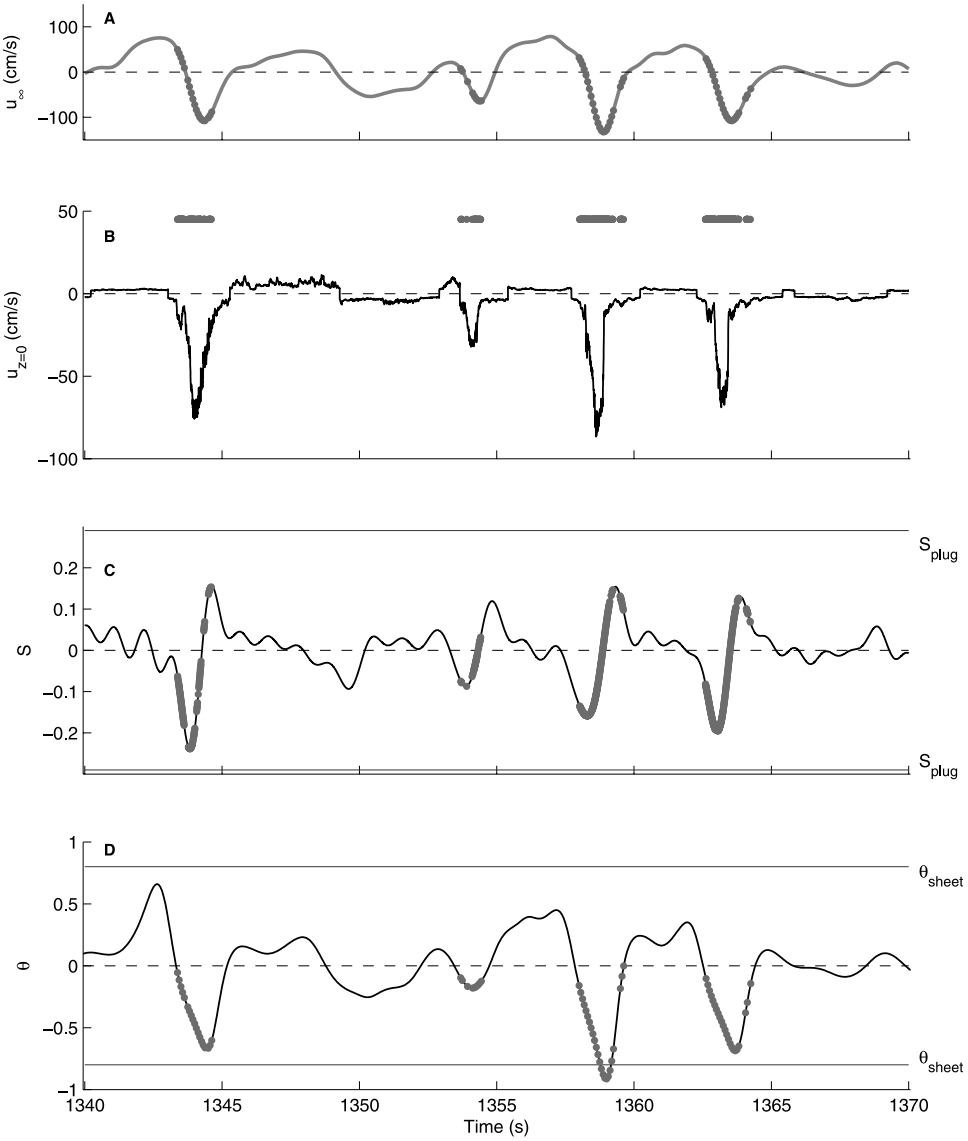

Figure 3. A comparison of the Sleath and Shields parameters for the given observations. (a and b) The observed free-stream and bed velocity measured at 10.5 cm and 0 cm above the intermittently still bed, respectively. (c) The instantaneous Sleath parameter, S(t), is a measure of pressure gradient induced sediment transport. Bed mobilizations are coincident with peaks in S(t). However, the critical limit for plug flow ($|S_\omega| > 0.29$) as specified by rigid lid laboratory tunnel experiments is never reached. (d) The instantaneous Shields parameter, θ, is a measure of shear-induced sediment transport. The critical limit for sheet-flow ($|\theta_{sheet-flow}| > \pm 0.8$) is approached several times and exceeded once. Instances of bed mobilization are qualitatively identified with instantaneous velocity magnitudes (at z = 0) of greater than 20 cm/s (red lines).

smaller than the 20∼30° phase shift predicted for purely sinusoidal waves. The boundary layer thickness and phase shift is more pronounced for the longer excursions present during offshore-directed flow than for the large accelerations but shorter durations present during the onshore-directed flow. Shear-induced transport roughly parameterizes grain destabilization with the shear stress applied over a single grain thickness. However, given that the momentum equation is forced with the free-stream acceleration, the bed stress exhibits some dependence on the pressure gradient. The critical limit for sheet-flow (θ = 0.8) was exceeded once and approached several times in the 30-second record. However, the bed mobilizations occurred well prior to peaks in the predicted Shields parameter and are therefore consistent with the pressure gradient forcing.

[13] Given the highly unsteady nature of the flow, the average statistics over the 256-second record are estimated with average distribution of S, θ, and $u(z = 0)$ at comparable wave phases (Figure 4). For this analysis, the wave-phase average is defined as the average quantity at comparable free-stream velocities and local accelerations. The third velocity sensor, which is at the approximate undisturbed bed level ($z = 0$), is used to identify incipient motion. Consistent with quasi-steady theory, the Shields parameter

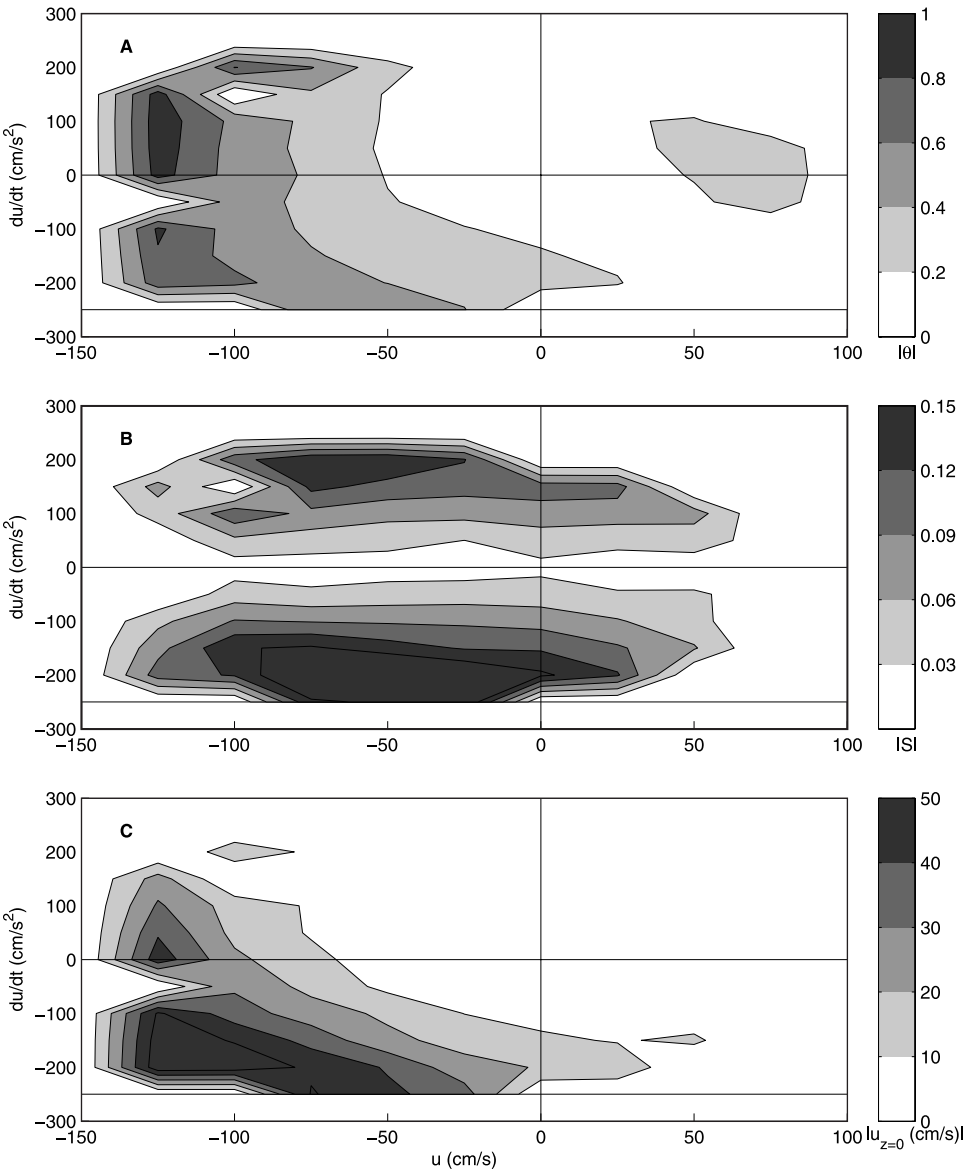

Figure 4. The distribution of the (a) Shields parameter, θ, and (b) Sleath parameter, S, are compared with the (c) incipient motion of the bed, $u(z = 0)$ at comparable wave phases. The wave phase for these random waves is characterized with the free-stream velocity and acceleration. The flow progresses in a clock-wise manner around the figure.

is largest near-bed the larger wave crests when the velocity is largest ($|U_o(t)| > 100$ cm/s). In contrast, the instantaneous Sleath parameter is largest during flow reversal from offshore- to onshore-directed flow when the free-stream acceleration is largest ($|dU_o(t)/dt| > 200$ cm/s^2). Incipient motion, as estimated with the velocity located at the undisturbed bed elevation, occurred during the accelerating phase prior to large wave crests and prior to peaks in the Shields parameter. These results are indicative of incipient motion induced by the horizontal pressure gradient of the normal stresses applied to the bed rather than the vertical gradient of the shear stress.

3. Discussion

[14] Observations of the mobile-bed layer dynamics in a large-scale wave flume by *Dohmen-Janssen and Hanes* [2002, 2005] provide us with an opportunity for comparison with the above observations. Observations of the water column velocity at 10 cm above the bed and the grain velocities within the mobile-bed sediment bed were obtained for both monochromatic skewed waves and wave groups. The monochromatic test runs (case mh) that was comparable with the Duck94 observations had a wave period of 6.5-seconds, a crest velocity of 109 cm/s, and a trough velocity of 72 cm/s [*Dohmen-Janssen and Hanes*, 2002]. The wave group test run presented in *Dohmen-Janssen and Hanes* [2005] had a wave period of 9.1 sec, a wave group period of 90 sec, peak crest velocities of 150 cm/s, trough velocities of 80 cm/s, and peak accelerations of near-bed 200 cm/s^2. The grain velocities were estimated with a correlation between two near-bed concentration sensors and was limited to estimates of the grain

velocities above an unspecified value. The observations show grain velocities within an intermittently still bed of 50–70% of the free-stream velocity. Within a single wave, the first estimate of grain velocities occurs during the accelerating phase of the onshore-directed flow when the free-stream velocity is between 30–70 cm/s. For the wave group observations [*Dohmen-Janssen and Hanes*, 2005], non-zero velocities are 70% of $u(z = 10)$ and occur for $u(z = 10) > 35$ cm/s when the peak acceleration is nearly 200 cm/s^2. The timing of the non-zero grain velocities and the magnitude of the grain velocities are consistent with the Duck94 observations.

[15] Although the shear and pressure gradient terms may act in concert to mobilize and transport sediment, there exists considerable difficulty in assessing the relative importance of the two mechanisms. If we re-arrange the force balance on the block of sediment given in *Sleath* [1999], sediment is mobilized when

$$|-\theta\frac{d_{50}}{h} - S(t)| > KC_b(1+\alpha) \tag{5}$$

where h is the block thickness, K (= 0.58) is the coefficient of friction, C_b (= 0.64) is the volumetric sediment concentration, and α is a coefficient. The Sleath parameter properly parameterizes the pressure gradient in the force balance, whereas the Shields parameter substitutes a single grain size for the unknown vertical length scale over which the bed stress is distributed. This formulation shows that as the depth of the mobile-bed layer increases, the relative importance of the pressure gradient also increases. Equation (5) suggests that instead of examining the critical values for shear- and/or pressure gradient induced mobilization, we should instead use equation (5) to specify the critical limit for motion. During strengthening flow phases, the two terms will combine to destabilize the bed, but during weakening flow phases the net result will be to stabilize the bed. This formulation is currently limited by a requirement to estimate the depth of movement, h, a priori.

4. Conclusions

[16] These observations provide the first field evidence of plug flow on natural beaches. The observed centimeter-scale bed mobilizations were coincident with large horizontal pressure gradients that result from short-period (O(5 s)) shallow water waves. The observations were obtained in 1.5 m of water when the near-bed horizontal velocity reached more than 1 m/s. The thickness of this mobile-bed layer is larger than shear-induced sheet-flow thicknesses and the initiation of the intermittently mobile-bed layer occurs during the transition from offshore- to onshore-directed flow. The mobile-bed thickness and timing of mobilization is consistent with the concept that pressure gradient induced transport plays a very significant role in incipient motion. Bed mobilization occurred for $S(t) > 0.1$, which is lower than the critical value observed in a rigid lid laboratory tunnel [*Sleath*, 1999]. Although the vertical velocities present in nature (but not reproduced in rigid-lid tunnels) may enhance the bed dilation, a horizontal force balance on a block of sediment suggests that incipient motion occurs when the shear and pressure gradient terms act in concert to exceed some threshold value. These results also suggest that during a weakening flow phase, the two terms may oppose one another and act to stabilize the bed. Horizontal pressure gradients induced by surface gravity waves provide an additional physical mechanism that provides for the onshore-directed transport of nearshore sediment under moderate wave conditions.

[17] **Acknowledgments.** We thank R. Beach for his guidance and involvement in the data collection and analysis. We also thank E. Gallagher for her valuable comments. Staff at the U.S. Army Corps of Engineers Field Research Facility provided logistical support for the instrument deployment. Funding for this effort was provided by the Office of Naval Research and the Andrew Mellon Foundation.

References

Bagnold, R. A. (1966), An approach to the sediment transport problem from general physics, *U.S. Geol. Surv. Prof. Pap.*, *422-1*, 231–291.

Bailard, J. A. (1981), An energetics total load sediment transport model for a plane sloping beach, *J. Geophys. Res.*, *86*(C11), 938–954.

Bowen, A. J. (1980), Simple models of nearshore sedimentation; beach profiles and longshore bars, in *The Coastline of Canada*, edited by S. B. McCan, *Pap. Geol. Surv. Can.*, *80-10*, 1–11.

Chang, Y. S., and D. M. Hanes (2004), Suspended sediment and hydrodynamics above mildly sloped long wave ripples, *J. Geophys. Res.*, *109*, C07022, doi:10.1029/2003JC001900.

Conley, D. C., and D. L. Inman (1992), Field observations of the fluid-granular boundary layer under near breaking waves, *J. Geophys. Res.*, *97*(C6), 9631–9643.

Dick, J. E., and J. F. A. Sleath (1991), Velocities and concentrations in oscillatory flow over beds of sediment, *J. Fluid Mech.*, *223*, 165–196.

Dohmen-Janssen, M., and D. M. Hanes (2002), Sheet flow dynamics under monochromatic nonbreaking waves, *J. Geophys. Res.*, *107*(C10), 3149, doi:10.1029/2001JC001045.

Dohmen-Janssen, M., and D. M. Hanes (2005), Sheet flow and suspended sediment due to wave groups in a large wave flume, *Cont. Shelf Res.*, *25*(3), 333–347.

Dohmen-Janssen, M., W. Hassan, and J. Ribberink (2001), Mobile-bed effects in oscillatory sheet flow, *J. Geophys. Res.*, *106*(C11), 27,103–27,115.

Drake, T. G., and J. Calantoni (2001), Discrete particle model for sheet flow sediment transport in the nearshore, *J. Geophys. Res.*, *106*(C9), 19,859–19,868.

Elgar, S., and R. T. Guza (1985), Observations of bispectra of shoaling surface gravity waves, *J. Fluid Mech.*, *161*, 425–448.

Engelund, F., and J. Fredsøe (1976), A sediment transport model for straight alluvial channels, *Nordic Hydrol.*, *7*, 293–306.

Foster, D. L., R. A. Beach, and R. A. Holman (2000), Field observations of the wave bottom boundary layer, *J. Geophys. Res.*, *105*(C8), 19,631–19,648.

Fredsøe, J., and R. Deigaard (1992), *Mechanics of Coastal Sediment Transport*, World Sci., Hackensack, N. J.

Fredsøe, J., K. H. Anderdsen, and B. M. Sumer (1999), Wave plus current over a rippled bed, *Coastal Eng.*, *38*, 177–221.

Gallagher, E. L., E. Elgar, and R. T. Guza (1998), Observations of sandbar evolution on a natural beach, *J. Geophys. Res.*, *103*(C2), 3203–3215.

Hanes, D. M., and A. J. Bowen (1985), A granular-fluid model for steady intense bedload transport, *J. Geophys. Res.*, *90*(C5), 9149–9158.

Henderson, S. M., J. S. Allen, and P. Newberger (2004), Nearshore sandbar migration predicted by an eddy-diffusive boundary layer model, *J. Geophys. Res.*, *109*, C06024, doi:10.1029/2003JC002137.

Hoefel, F., and S. Elgar (2003), Wave-induced sediment transport and sandbar migration, *Science*, *299*, 1885–1887.

Horikawa, K., A. Watanabe, and S. Katori (1982), Sediment transport under sheet flow conditions, in *Proceedings of 18th Conference on Coastal Engineering*, pp. 1335–1352, New York.

Hsu, T., and D. Hanes (2004), Effects of wave shape on sheet flow sediment transport, *J. Geophys. Res.*, *109*, C05025, doi:10.1029/2003JC002075.

King, D. B. (1991), Studies in oscillatory flow bedload sediment transport, Ph.D. thesis, Univ. of Calif., San Diego.

Madsen, O. S. (1974), Stability of a sand bed under breaking waves, in *Proceedings of 14th Conference on Coastal Engineering*, pp. 776–794, New York.

Nielsen, P. (1992), *Coastal Bottom Boundary Layers and Sediment Transport*, World Sci., Hackensack, N. J.

Ribberink, J. S., and Z. Chen (1993), Sediment transport of fine sand under asymmetric oscillatory flow, *Rep. H840, Part VII*, Delft Hydraul., Delft, Netherlands, Jan.

Shields, A. (1936), Anwendung der anhlichkeitsmechanik und turbulenzforschung auf die geschiebebewegung, *Mitt. Preuss Versuchsanstalt fur Wassebaur und Schiffbau*, *26*.

Sleath, J. F. A. (1994), Sediment transport in oscillatory flow, in *Sediment Transport Mechanisms in Coastal Environments and River*, edited by M. Belorgey, R. D. Rajaona, and J. F. A. Sleath, World Sci., Hackensack, N. J.

Sleath, J. F. A. (1999), Conditions for plug formation in oscillatory flow, *Cont. Shelf Res.*, *19*, 1643–1664.

Sumer, B. M., A. Kozakiewicz, J. Fredose, and R. Diegaard (1996), Velocity and concentration profiles in sheet flow layer of movable bed, *J. Hydraul. Eng.*, *122*(10), 549–558.

Terrile, E., A. J. H. M. Reniers, M. J. F. Stive, M. Tromp, and H. J. Verhagen (2005), Incipient motion of coarse particles under regular shoaling waves, *Coastal Eng.*

Thornton, E. B., R. T. Humiston, and W. Birkemeier (1996), Bar-trough generation on a natural beach, *J. Geophys. Res.*, *101*, 12,097–12,110.

Wilcox, D. C. (1993), Comparison of two-equation turbulence models for boundary layers with pressure gradient, *AIAA J.*, *31*(9), 1414–1421.

Zala Flores, N., and J. F. A. Sleath (1998), Mobile layer in oscillatory sheet flow, *J. Geophys. Res.*, *103*(C6), 12,783–12,793.

Zyserman, J., and J. Fredsøe (1994), Data analysis of bed concentration of suspended sediment, *J. Hydraul. Eng.*, *120*(9), 1021–1042.

A. J. Bowen, Department of Oceanography, Dalhousie University, Halifax, NS, Canada B3H 4J1.

D. L. Foster and P. Natoo, Department of Civil and Environmental Engineering and Geodetic Science, Ohio State University, Columbus, OH 43210-1275, USA. (foster.316@osu.edu)

R. A. Holman, College of Oceanic and Atmospheric Sciences, Oregon State University, Corvallis, OR 97331, USA.